Chapter 6
Multifunctional Quantum Dot-Based Nanoscale Modalities for Theranostic Applications

Bowen Tian

Abstract Quantum dots (QD) have shown unprecedented fluorescent properties that are capable of revolutionising the field of optical imaging. Due to its unique fluorescent properties, QD have been extensively explored as imaging reagents for the investigation of various biological behaviours in vitro and in vivo. The design and engineering of multifunctional, QD-based modalities have recently attracted enormous interest for simultaneous imaging and therapy. The presence of QD as imaging agent in the theranostic modalities allows for the visualisation of their behaviour in real time and, thus, allows the monitoring of biodistribution, the percentage of drugs in the target site and regional uptake of the drug, as well as clearance from the body in real time, after systematic administration. All this information obtained from QD-based theranostic modalities is believed to be greatly helpful for the better understanding of biological behaviours and further optimization of novel therapeutic modalities, in preclinical and clinical investigations. This chapter attempts to give a brief overview of QD ranging from fundamental knowledge to multifunctional QD-based theranostic modalities for gene therapy, chemotherapy and photodynamic therapy.

Keywords Multifunctional modality • QD • Theranostics • Cancer therapy and imaging • Nanomedicine • Optical imaging

B. Tian (✉)
Laboratory of Biophysics and Surface Analysis Division, School of Pharmacy, University of Nottingham, Nottingham NG7 2RD, UK
e-mail: bowen.tian@nottingham.ac.uk

Z. Dai (ed.), *Advances in Nanotheranostics I*, Springer Series in Biomaterials Science and Engineering 6, DOI 10.1007/978-3-662-48544-6_6

6.1 Quantum Dot

6.1.1 Optical Imaging

Optical imaging is a non-invasive, reliable and highly sensitive technique, with nanometre-scale resolution for exploring various biological activities in the life sciences [1–4]. Fluorescent imaging methods rely on the detection of emission light from fluorophores, when the fluorophores are excited by using a light source with specific wavelength. Therefore, the fluorescent properties of the fluorophores are of utmost importance in the successful application of such techniques. Ideal fluorophores require strong emission, high photostability, no toxicity and ease of chemical modification (e.g. conjugation with targeting ligands). Furthermore, for in vivo imaging, both excitation and emission light require efficient penetration through the tissues. NIR (near infrared, 700–1000 nm) imaging [5, 6] has recently attracted enormous interest, due to deep-tissue fluorescence imaging, compared to short light (<700 nm). NIR offers image-guided operation in the clinic [6–8]. The recent development of fluorescence molecular tomography [9] and photoacoustic tomography [10] will promote the applications of optical imaging in the life sciences.

The fluorophores are divided into inorganic (QD [11], graphene QD [12], gold nanoparticles [13]), carbon nanotube [14], hybrids (lanthanide chelates [15]) and organic dyes (cyanine [16]). One of the most promising fluorescent probes is the quantum dot, which can revolutionise the fluorescent detection techniques given QD's unprecedented superior fluorescent properties, compared to traditionally used fluorescent dyes.

6.1.2 Quantum Dot Fluorescence Characteristics

QD are fluorescent, semiconductor, nanocrystals with typical diameters ranging from 1 to 10 nm [17]. Due to their superior fluorescence characteristics in comparison with traditionally used organic dyes, QD have been extensively used for a variety of biological investigations in vitro and in vivo [18–23]. Their unique fluorescent properties are characterised by size-dependent colour, pronounced photostability and sharper emission spectra and much broader absorption spectra.

- First, QD are characterised by their unique size and/or composition-dependent colour. This allows the design and synthesis of QD with customised colour, such that it is visible to infrared for specific applications [24–27].
- Second, QD have shown pronounced photostability. The growth of a passivation shell (e.g. zinc sulphur) around it can further improve their photostability for long-term and stable fluorescent imaging [17, 28, 29]. These core/shell QD, for example, CdSe/ZnS, are excellent fluorescent probes for long-term fluorescence imaging applications.

- Third, QD possess sharper emission spectra and much broader absorption spectra, compared to organic dyes. This unique fluorescent characteristic enables simultaneous imaging of QD of different colours, using one single excitation light source [26, 30–32]. In practice, this has been used for multiplex imaging to track cancer cell metastasis [33, 34] and differentiate tumour tissue [35] in vivo.
- Fourth, QD are much brighter and robust against photobleaching [36, 37]. Under the exposure of excitation light, QD can maintain stable fluorescence for a much longer time than organic dyes.

All these fluorescent characteristics form the basis for QD-based imaging applications for various biological studies; for example, for cell tracking [38–40], tumour vessels [41, 42], lymph nodes [43, 44] and solid tumours [19, 45, 46] in vivo.

6.1.3 Quantum Dot Synthesis and Composition

High-quality monodisperse QD was first reported by Bawendi and co-workers in 1993 [47]. Their synthetic method controlled well the colloidal stability of QD to maintain its monodispersed status and, therefore, elucidated its unique fluorescent characteristics, including size-dependent fluorescence for the first time. CdSe QD are the mostly widely used in biological applications due to a well-established synthetic chemistry [21]. In a typical CdSe QD synthesis, selenium (commonly trioctylphosphine selenide or tributylphosphine selenide) and cadmium precursors (dimethylcadmium or cadmium oleate) are injected into a high-temperature (300 °C) organic solvent containing coordinating polymers (trioctylphosphine oxide or hexadecylamine) [28, 47, 48]. Selenium and cadmium precursors are fast reacting to form the CdSe nucleus, and, in the meantime, coordinating ligands are attached to the CdSe nucleus surface to maintain colloidal stability. Cadmium and selenium continuously grow on the existing CdSe core, until the growth of QD reaches a desired size as monitored by the absorption spectrum [49]. A ZnS shell can be grown on the CdSe surface to enhance QD photoluminescence efficiency [17], stability against oxidative photobleaching [17, 28, 29] and colloidal stability [50]. Due to coordinating polymer coating (e.g. trioctylphosphine oxide, TOPO), QD are extremely hydrophobic and require further engineering to be dispersible in water.

With the development of QD synthetic chemistry, QD have been synthesised in aqueous solutions, high-temperature organic solvents and solid substrates [21] using various materials, mainly from II–IV (e.g. ZnS and CdS) and III–V (e.g. InP and InAs) group semiconductor materials. Alloyed QD tunes emission wavelengths by manipulating compositions [24, 26]. Cadmium-free QD of $CuInS_2$ emits fluorescence in the NIR range and greatly minimises toxicity compared to traditionally used cadmium containing QD (e.g. CdSe) [51]. Many more novel types of QD, with different properties, are under development, including graphene QD [52, 53] and nitrogen-rich QD [54].

6.1.4 Quantum Dot Solubilisation and Functionalisation

Both Nie and Alivisatos groups first engineered water-soluble QD for biological applications. This was achieved by coating hydrophobic QD with mercaptoacetic acid [55] or silica [56]. For the engineering of water-soluble QD, two typical methods have been developed, namely, ligand exchange and amphiphilic polymer coating.

For ligand exchange, bifunctional ligands composed of a thiol group at one end are used. The thiol group is used to replace hydrophobic coordinating polymers (e.g. trioctylphosphine oxide (TOPO)), due to a stronger binding affinity to cadmium. The other end of the bifunctional ligand is normally composed of a hydrophilic group, which is exposed outside to interact with hydrophilic molecules (e.g. water) [36, 55, 56]. A variety of thiol-containing molecules have been used to make water-soluble QD following the ligand-exchange strategy, including (1) thiol-containing chemical molecules, such as mercaptoacetic acid (MAA), dihydrolipoic acid and mercaptopropyltris (methoxy) silane (MPS) [36, 55, 56], (2) peptides [57], (3) dendron [58], (4) oligomeric phosphine [59] and (5) silica [60]. It is notable that the replacement of TOPO coating successfully makes water-soluble QD, but it has been found to result in unfavourable effects on QD fluorescence and colloidal stability [55, 56, 61].

For amphiphilic polymer coating, their hydrophobic domain is used to interact with hydrophobic coordinating polymers, leading to the formation of an amphiphilic polymer coating around TOPO-capped QD. A variety of amphiphilic polymers have been used following this strategy, such as phospholipid micelles, triblock copolymer and amphiphilic diblock. Moreover, amphiphilic polymer coating has shown minimal effect on QD fluorescence and colloidal stability, compared to ligand exchange [19, 39, 62, 63] and, thus, has been the most commonly adopted approach for engineering stable, water-soluble QD. However, it is also notable that the formation of amphiphilic polymer coating around QD leads to a size increase [21].

For the functionalisation of QD, a variety of methods have been utilised, such as electrostatic absorption, covalent conjugation and streptavidin-biotin linking [21, 55, 64]. QD have been functionalised using various molecules for biological applications, such as antibodies [65–69], peptides [41, 42, 70], endosome-disruptive polymers [71], aptamers [72–75], radionuclides [76–78], magnetic resonance imaging (MRI) agents [79, 80] and therapeutic molecules [81–84]. Moreover, polyethylene glycol (PEG) has been successfully used to prolong QD blood circulation half-life in vivo and minimise immunogenicity and cytotoxicity [43, 85–87]. Figure 6.1 shows a schematic structure of functionalised QD for in vivo targeted imaging.

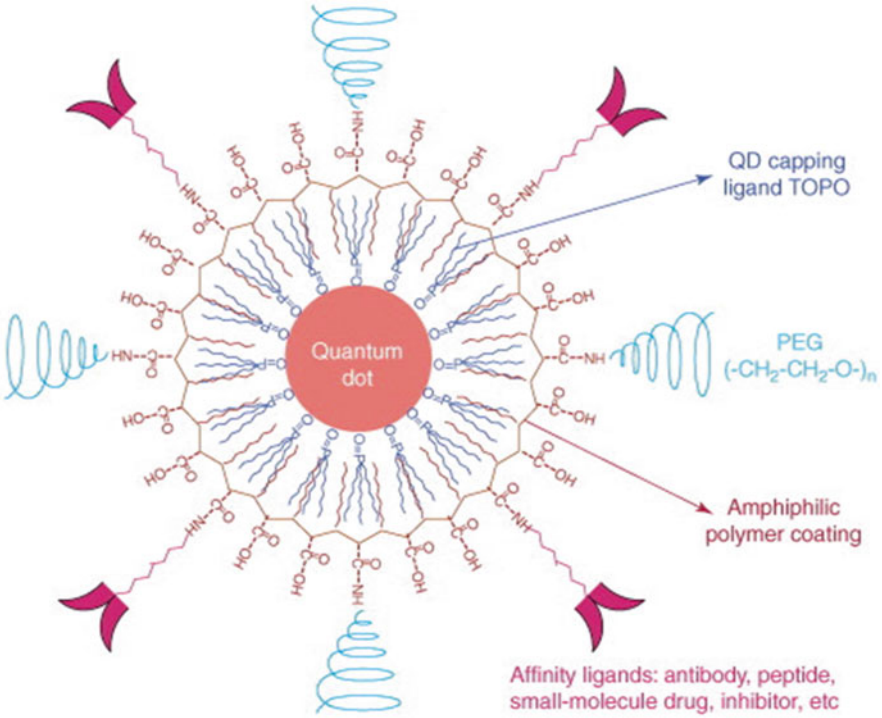

Fig. 6.1 The structure of a multifunctional QD. Schematic illustration showing the capping ligand TOPO, encapsulating copolymer layer, tumour-targeting ligands (such as peptides, antibodies or small-molecule inhibitors) and polyethylene glycol (PEG) (Reprinted from Ref. [87], copyright 2005, with the permission from Elsevier)

6.1.5 Quantum Dot in Biomedical Application

QD have been successfully used in fluorescent-based imaging and diagnostic applications in vitro and in vivo, for instance, (a) in vitro cell labelling [38, 39], fluorescent nanoprobes [88, 89] and biosensors based on the fluorescence resonance energy transfer (FRET) [90, 91] and (b) in vivo tumour vascular imaging [41, 92], tracking cells [40, 62, 93], lymph nodes [43, 44, 94] and solid tumours [95–97]. Due to the broad excitation spectra of QD, simultaneous detection using different coloured QD has enabled multiplex imaging to be used for tracking cancer cell metastasis [33, 34] and differentiating tumour tissue [35] in vivo.

Nowadays, fluorescent imaging using QD in vivo offers direct visualised evidence, but is mostly semi-quantitative. For accurate quantitative analysis, QD require the combination of fluorescence with other detection methods (e.g. radiolabelling). Recently, QD have been engineered such that they are equipped with magnetic [80, 98], paramagnetic [99] or radioactive properties [76, 78, 100], for more sensitive and quantitative diagnostic applications. Such dual-function nanoprobes

allow detection using multiple techniques, such as magnetic resonance imaging (MRI), positron emission tomography (PET) and single-photon emission computed tomography (SPET), along with fluorescence techniques such as IVIS camera [76, 99, 101]. For instance, tumour targeting of ^{64}Cu-labelled QD was directly visualised by NIR fluorescence imaging of QD. With radiolabelling of ^{64}Cu, the tumour-targeting efficiency of the QD was accurately quantified by the means of ultrahigh sensitivity of the radionuclide using PET [77]. Interestingly, Cai et al. (2007) further found that the tumour-to-muscle ratios obtained from NIR imaging were in agreement with PET analysis for certain organs, for example, the liver and spleen [77].

6.1.6 Quantum Dot Biodistribution and Pharmacokinetics In Vivo

Most studies have shown that QD are rapidly taken up by the reticuloendothelial system (RES), with high accumulation in the liver and spleen after systemic administration [100, 102–106]. Studies, so far, have shown that PEGylation, size and surface coating are the three critical factors which determine QD biodistribution and pharmacokinetics.

With respect to PEGylation, Ballou et al. have reported, by non-invasive fluorescent imaging, that the QD surface modified with PEG_{5000} (5,000 Da) greatly prolongs blood circulation half-life ($t_{1/2} = 140$ min), compared to short PEG_{750} and PEG_{3400} ($t_{1/2} < 12$ min) [102]. However, high uptake by the liver, spleen, lymph nodes and bone marrow was observed up to 4 months [102]. Consistently, PEG_{5000}-conjugated QD achieved long blood circulation half-life and, thus, facilitated targeting to the desired tissues in vivo [19, 45]. In 2009, Choi and co-workers reported that the biodistribution and pharmacokinetics of QD can be manipulated by surface modification using different lengths of PEG [103]. Choi et al. (2009) found that QD conjugated with PEG2 (two monomers) primarily accumulate in the liver; PEG8 accumulate in the pancreas; PEG3 and PEG4 are excreted via renal clearance and PEG22 circulate in the vasculature.

With respect to QD size, Fischer et al. (2006) have reported that QD linked to proteins (bovine serum albumin, BSA), 80 nm in diameter, were prominently accumulated in the liver compared to small QD (cross-linked with lysine, 25 nm in diameter) (99 % ID/g vs. 36 % ID/g, respectively) after 90 min postinjection [104]. This finding indicates that the interaction between QD and blood proteins leads to QD size increase and thus would result in rapid clearance by the RES system in vivo, similar to QD-BSA conjugates. In 2007, Choi et al. reported that zwitterionic QD showed biodistribution and clearance in a size-dependent manner. QD of 5.5 nm in hydrodynamic diameter can be efficiently excreted via urine, whereas larger QD (8.65 nm in diameter) showed high liver uptake but no urine clearance [105].

Moreover, it is evident that the extent of QD migration in the lymphatic system depends on QD size. QD with an average diameter of 15–20 nm migrate rapidly to

the sentinel lymph nodes (SLN), but primarily accumulate in the first lymph node, when administrated through subcutaneous, intradermal, intraperitoneal and intraparenchymal routes [20, 107–112]. In comparison, smaller QD with mean diameter of 9 nm migrate further into the lymphatic system up to five nodes [112].

Very recently, Schipper et al. (2009) attempted to investigate the effect of particle size, surface coating and PEGylation on QD biodistribution and pharmacokinetics in nude mice after intravenous administration [106]. Schipper et al. (2009) injected polymer- or peptide-coated ^{64}Cu-labelled QD, 2 and 12 nm in diameter, with or without surface-conjugated PEG_{2000}, and did the analysis using both PET and ICP-MS (inductively coupled plasma mass spectrometry). It was found that PEG_{2000} conjugation to the large QD (12 nm) surface delayed accumulation in the liver and spleen, whereas such delayed uptake by the RES system was not observed from PEG_{2000}-conjugated small QD (2 nm). Moreover, unlike polymer coating, peptide coating enhanced QD excretion, with higher accumulation in the bladder observed from small QD compared to large QD (7.6 % ID/g vs. 2.5 % ID/g, respectively).

Overall, it can be seen that QD biodistribution and pharmacokinetics in living animals are affected by many factors, such as hydrodynamic diameter, surface charge, PEG length and the route of administration. Furthermore, it has been shown that only very small neutral and zwitterionic QD (<5.5 nm in diameter) can be excreted efficiently via urine [103, 105], while larger QD have a tendency to accumulate in the body [104, 113], which will consequently raise the toxicity issue of QD.

6.1.7 Toxicity Profiles of Non-functionalised Quantum Dot

The concern over QD toxicity is mainly derived from their intrinsic core compositions, such as cadmium (e.g. CdSe and CdTe). The correlation between cytotoxicity and free Cd^{2+} ions has been established [60, 114, 115] with the occurrence of significant cell death in the range of 100–400 μM Cd^{2+} ions [43]. Derfus et al. reported that CdSe QD are toxic due to the release of cadmium ions (Cd^{+2}) initiated upon photolysis and/or oxidation. This was evidenced by the blue shift in QD absorbance spectra due to size deduction and subsequent release of Cd^{+2} [114]. Furthermore, the process in the production of Cd^{+2} ions has been found to be accompanied by the formation of reactive oxygen species (ROS), such as singlet oxygen (O_2^-), due to QD electron donation to oxygen [105, 116, 117]. Cho et al. observed significant lysosomal damage due to the presence of both Cd^{+2} ions and ROS after a 24-h cell incubation [118].

So far, studies have demonstrated that QD cytotoxicity is attributed to the use of core QD (e.g. CdTe), without ZnS coating, especially those solubilised by the ligand-exchange method, such as mercaptopropionic acid (MPA-QD) [77, 117, 119–121], mercaptoacetic acid (MAA-QD) [114], mercaptoundecanoic acid (MUA-QD) [121], cysteamine (QD-NH_2) [118, 119] and thioglycerol (QD-OH) [115]. These ligands have weak electrostatic interactions with QD and are found to

detach from the QD surface [122, 123]. Such ligand detachment may be worse in harsh conditions like endosomal compartment [56] leading to severe cell death [60, 105, 117, 119, 120].

In comparison, QD coated with ZnS shell (CdSe/ZnS [114] and CdTe/ZnS [118]) can protect the QD core from oxidation, thereby minimising Cd^{+2} leakage and subsequently reducing the QD-induced cytotoxicity [60, 118, 119]. Moreover, QD solubilised with a stable coating, such as silica, were shown to be non-toxic up to a high Cd^{+2} surface concentration [60] and highly resistant to chemical and metabolic degradation [124], as well as non-toxic even if translocated to the cell nucleus [125], or at the gene level [86].

Nowadays, most biological investigations have selected core/shell QD with stable amphiphilic polymer coating, used at relatively low concentrations (nmol to pmol). Therefore, no obvious toxicity has been observed from QD. For example, *Xenopus* embryos [62] and zebrafish embryos [126] microinjected with QD did not exhibit any sign of toxicity until a high concentration was used, leading to abnormalities in the embryos. Furthermore, QD injected systemically in mice and rats has shown no apparent toxicity in pmol-nmol range, even after 4 months [43, 104, 127, 128]. Moreover, large animals (e.g. Yorkshire pigs) injected with 200–400 pmol of QD for the sentinel lymph node (SLN) mapping showed no physiological changes in the heart rate, blood pressure and oxygen level even after several hours [20, 109–111].

Overall, cytotoxicity studies have shown that the toxicity of QD can be minimised by coating with ZnS shell and solubilising using amphiphilic polymer coating, especially when a low dose is used during the period of the experiment. However, heavy metal containing (e.g. cadmium) QD composition would be a major obstacle for clinical use.

6.2 Quantum Dot for Theranostic Applications

6.2.1 Quantum Dot-Based Gene Therapy Modalities

Gene therapy is one of the most promising solutions to various formidable diseases, including cancer. However, to achieve effective gene therapy requires the efficient and specific delivery of nucleic acid inside of cellular compartments (e.g. nucleus). Various biological barriers, therefore, need to be overcome to deliver nucleic acid inside of cells. Moreover, the release of nucleic acid from delivery vectors inside of the cells is guaranteed. This is a complicated process, which is currently not yet fully understood. QD offers excellent fluorescent properties in studying various processes associated with nucleic acid delivery, including complexation, and the release and intracellular trafficking of nucleic acid complexation. The fluorescence resonance energy transfer (FRET) phenomenon is used to construct the QD-FRET pair for the investigation of nucleic acid delivery.

The FRET effect is used to monitor fluorescent changes in a fluorescent molecule pair, including a donor and an acceptor. Fluorescent changes are due to the distance alteration in nanoscale (called the Forster radius, typically several nanometres) between the pair. For example, when a donor molecule and an acceptor molecule are approaching each other within Forster radius, the receptor starts to absorb energy from the donor, and as a result, the donor loses its fluorescence. When the two molecules are separating from each other (beyond Forster radius), the receptor cannot absorb energy from the donor, and as a result, the donor recovers fluorescence to a normal level.

The advantage of constructing the QD-FRET pairs is that QD stable fluorescent properties, against photobleaching, allows stable and long-term fluorescent imaging of nucleic acid delivery, release and related behaviours. In a typical example of QD-FRET pairs, QD-labelled pDNA forms complexation with fluorescently Cys5-labelled chitosan [129]. The FRET effect allows the monitoring of the integrity of the complexation inside of cells (by observing Cys5 fluorescence due to energy transfer from QD-labelled pDNA), whereas released pDNA only shows QD fluorescence. Moreover, intracellular trafficking was conducted in a highly sensitive and quantitative way. Following the same FRET strategy, similar studies have been carried out to investigate DNA condensation and stability [130], as well as DNA polymer complexation [131]. It is notable that photoactivation of QD is often accompanied with the production of reactive oxygen species (ROS), which leads to the breakage of DNA in QD-DNA conjugates [132]. This could offer a novel strategy to induce the release of DNA from QD upon light activation for controlled delivery of DNA inside of cells.

Apart from constructing QD-FRET pairs with DNA, QD is also explored as a delivery vector for DNA delivery. QD-loaded micelles carrying functional groups (e.g. maleimide) have been directly conjugated with pDNA molecules [133]. Such pDNA-QD micelle conjugates allow stable monitoring of pDNA intracellular trafficking, by QD fluorescence, for a long period of time. Moreover, pDNA-QD conjugates can successfully deliver pDNA inside of cells and result in the expression of reporter proteins, relevant to pDNA control. Positively charged QD have been used to complex with DNA due to electrostatic interactions [134]. Such a QD-DNA complex demonstrated a DNA release induced by glutathione in a concentration-dependent manner. This is probably due to the fact that glutathione has preferential interactions with the QD surface, leading to QD's surface charge change and, thus, release of DNA [134]. Near-infrared QD has been used to track the biodistribution of QD-DNA complexes in vivo [135]. The QD-DNA complex demonstrated a high accumulation in the lung, initially, followed by fast redistribution from the lung to the liver. QD control, however, showed a predominant accumulation in the liver straightaway. Furthermore, after weeks postinjection, QD fluorescent signals were still detectable due to QD's excellent photostability.

QD has been explored to investigate the process of small interference RNA (siRNA) delivery. The typical process for siRNA delivery, including delivery siRNA into cells, release siRNA and gene knockdown, normally takes longer than 24 h since post-administration. Over this period of time, traditionally used organic dye

could suffer from significant fluorescence loss due to photobleaching and is, thus, not suitable for long-term monitoring of siRNA delivery [136]. In comparison, QD offers significant improvement in terms of photostability and, thus, has been extensively used to explore various processes related to siRNA delivery.

Cationic liposomes have been used to co-complex both QD and siRNA by simple mixing [137]. This study demonstrates the monitoring of siRNA delivery inside of cells, as well as an improvement in gene silencing, but suffers from an adverse effect on the size increase of the complex in comparison to the liposome control. Both siRNA and a tumour-targeting peptide have been covalently conjugated to the surface of PEGylated QD [136]. Such targeted nanoconstructs can be internalised by cancer cells and achieve efficient gene silencing. Moreover, siRNA conjugation to QD, using a cleavable linker, was found to improve the gene silencing effect due to the enhanced release of siRNA inside of cells, compared to a non-cleavable linker. Antibody-targeted chitosan nanoparticles encapsulating QD inside was complex with siRNA on the surface [138]. By monitoring QD fluorescence, such a multifunctional delivery system demonstrated an enhanced cellular uptake in cancer cell lines that overexpressed certain receptors. The siRNA-QD conjugates have been engineered by two different linking strategies: (a) a disulphide bond, which allows cleavage to release siRNA inside of cells, and (b) a covalent bond, to form stable siRNA-QD conjugates for monitoring siRNA delivery [139]. Two targeting ligands are conjugated on the surface of siRNA-QD conjugates, to ensure efficient cellular uptake (e.g. RGD peptide targeting) and effective gene silencing through HIV-Tat peptide. By monitoring QD fluorescence, intracellular trafficking can be monitored in real time, and, more importantly, such targeted siRNA-QD conjugates achieved therapeutic knockdown of specific proteins in brain tumour cells.

Peptide-QD conjugates have been explored as delivery vectors for simultaneously monitoring intracellular transportation and delivery of siRNA into cells. Cell-penetrating peptide conjugated QD are used to complex with cy3-labelled siRNA [140]. This study demonstrated successful intracellular delivery and cellular distribution of siRNA in the cells. However, the complex was found to be entrapped in the endosome. To release siRNA from the endosome, acid neutralisation of the endosome as well as destabilisation of such peptide-QD-siRNA complexes were achieved by the addition of chloroquine to the cell culture environment. The addition of chloroquine was found to lead to a successful redistribution of siRNA to the cytoplasm from the endosome. The engineering of QD-based delivery systems for siRNA delivery can improve gene silencing by up to 20-fold, compared to traditionally used transfection agents [141]. It is also notable that such QD-siRNA complexes can achieve gene silencing in the presence of serum, whereas traditionally used gene transfection agents need to work in serum-free environments. Such dramatic improvement is owing to a proton sponge effect, which is achieved by grafting equal amounts of carboxylic and amine groups on the QD surface. Moreover, fluorescence microscopy study has revealed that QD-siRNA complexes fast stick to the cell membrane, followed by internalisation and accumulation in the area outside of the cell nucleus, by monitoring QD fluorescence. The same group reported that

amphiphilic polymer amphipol-coated QD (with both carboxylic and amine groups) can achieve efficient siRNA delivery, irrespective of the presence of serum [142].

6.2.2 *Quantum Dot-Based Chemotherapy Modalities*

The engineering of theranostic modalities integrated with imaging and therapy into one unit has attracted enormous interest for cancer [143–146]. The presence of QD as an imaging agent in the theranostic modalities allows for the visualisation of their behaviour in real time. QD could allow the monitoring of biodistribution, the percentage of drugs in the target site, the regional uptake of the drug as well as the clearance from the body in real time, after systematic administration. All this information is believed to be greatly helpful for better understanding biological behaviours and for the further optimization of novel therapeutic modalities, in preclinical and clinical investigations.

For the engineering of QD theranostic modalities, QD can be directly surface conjugated with therapeutic molecules and targeting ligands [143–145]. One of the most successful QD-based theranostic modalities is reported by Bagalkot et al. in 2007, who covalently conjugated PSMA-targeted aptamers to the surface of hydrophilic QD and allowed doxorubicin loading through intercalation with the aptamers [145]. In this QD-aptamer(Apt)-doxorubicin(Dox) conjugates, QD and Dox formed a FRET pair (donor-receptor) and the loading of Dox quenched the QD fluorescence. This multifunctional QD demonstrated enhanced therapeutic effect in the targeted cells (LNCAP), and the gradual recovery of QD fluorescence inside of the cells indicated Dox release. Such theranostic modality showed promise for cancer targeting, imaging, therapy and traceable drug delivery simultaneously in vitro.

Alternatively, nanoscaled delivery systems (e.g. liposomes [96, 147–150], micelles [62, 151] and carbon nanotubes [152, 153]) can be used as a platform for the construction of QD theranostic modalities [144, 146]. Liposomes are the most established nanoscaled delivery systems. By the use of liposomes as a platform, various targeting ligands, diagnostic and therapeutic agents of interests can be integrated into liposomes for cancer imaging and therapy. This is particularly the case when liposome-QD hybrid constructs are successfully engineered. For example, Weng et al. (2008) covalently conjugated both anti-HER2-targeted scFv and hydrophilic QD to the liposome surface and loaded doxorubicin into the aqueous core of the liposomes for cancer imaging and therapy [146]. By tracking QD fluorescence, high drug delivery into (MCF-7/HER2) tumour in vivo was evidenced by the visualisation of strong QD fluorescence (14 % of total body fluorescence) in the tumour site after systemic administration. However, the conjugation of QD directly to the liposome surface has an adverse effect on the size of the whole structure. This was evidenced by the fact that QD-conjugated liposomes showed a decrease in blood circulation half-life, compared to liposome control (without QD).

Both Vogel and Kostarelos have proposed the engineering of lipid-QD hybrid, by the incorporation of hydrophobic QD (2 nm in diameter) into the lipid bilayer of

liposomes [147, 148, 150]. This is a straightforward method to make water-soluble QD. The lipid-QD hybrid engineered using cationic lipids has been used to label cells effectively in vitro and in vivo. Moreover, the lipid-QD hybrid can be used as a modular platform to load anticancer drugs (e.g. doxorubicin) into the aqueous core, and their surface can be further functionalised with targeting ligands for targeted cancer theranostics. The successful engineering of lipid-QD hybrids represents a feasible way to engineer multimodal nanoconstructs, for the development of personalised medicine. Such hybrids not only combine the unique fluorescent properties of QD with the physicochemical and pharmacokinetics of liposomes into one single vesicle but also allow further surface modification with polyethylene glycol and various targeting ligands (e.g. antibody).

Alternative multifunctional modalities can be engineered by simultaneous encapsulation of Dox, QD and magnetic nanoparticles into PEG-lipid micelles, for combined MRI and fluorescent imaging as well as cancer therapy [154]. Tumour accumulation of such modalities was confirmed by both fluorescent and MRI imaging after 20-h administration. Recently, the anticancer drug daunorubicin was reported to complex with anionic QD (3-mercaptopropionic acid coated) inside of cells, which could overcome multidrug resistance and improve the therapeutic effect in leukaemia cell lines [155].

6.2.3 Quantum Dot-Based Photodynamic Therapy Modalities

Photodynamic therapy (PDT) is the use of a specific light to activate photosensitisers (PS), in order to produce a toxic effect on certain cells and organs (e.g. tumour). For quantum dot, the exposure of excitation light produces both QD fluorescences and, in the meanwhile, leads to the production of reactive oxygen intermediates (ROI) to cause cell toxicity for simultaneous photodynamic therapy and imaging [156–158]. Photoactivation of QD is often accompanied by the production of ROI, which could lead to the breakage of DNA in the QD-DNA conjugates [132]. In the presence of antioxidant scavengers (e.g. N-acetylcysteine), such ROI-induced cell toxicity can be suppressed significantly [120]. It is also notable that QD by itself as photosensitisers cannot produce ROI for efficient cell toxicity.

An alternative strategy has been explored to use QD to enhance the toxicity of conventional photosensitisers, by taking advantage of the fluorescence resonance energy transfer (FRET) effect. QD can be used as a delivery platform for photosensitisers due to large surface area, efficient energy transfer and photostability, for improved photodynamic therapy. For example, the complexation between QD and photosensitiser (e.g. chlorin e6) increases the photodynamic therapy by twofold compared to chlorin e6 alone [157]. This was thought to be due to enhanced energy transfer from QD to the photosensitiser through the FRET effect.

6.3 Conclusion

QD has been used for the engineering of multifunctional theranostic modalities, for the investigation of various biological behaviours, including gene therapy, chemotherapy and photodynamic therapy. For gene therapy, QD allows the monitoring of complexation stability, release and intracellular trafficking inside of cells. For chemotherapy, QD allows the monitoring of the release of the drug inside of the cells and tracing nanoscaled delivery vectors' (e.g. liposome) behaviours, in vivo, including biodistribution and tumour accumulation. For photodynamic therapy, QD can be successfully used as an energy donor to enhance the toxicity of conventional photosensitisers. All these successes are attributable to QD's superior fluorescent properties. Although the concerns regarding QD toxicity could delay their clinical applications, QD as imaging agents are very useful for various biological studies and in vitro sample analysis. With the development of novel water-soluble and cadmium-free QD, the applications of QD-based theranostic modalities could offer useful tools for the investigation and optimization of novel therapeutic agents in clinical applications.

References

1. Byrne WL, DeLille A, Kuo C et al (2013) Use of optical imaging to progress novel therapeutics to the clinic. J Control Release 172:523–534
2. Ntziachristos V (2010) Going deeper than microscopy: the optical imaging frontier in biology. Nat Methods 7:603–614
3. Pan D, Caruthers SD, Chen J et al (2010) Nanomedicine strategies for molecular targets with MRI and optical imaging. Future Med Chem 2:471–490
4. Stender AS, Marchuk K, Liu C et al (2013) Single cell optical imaging and spectroscopy. Chem Rev 113:2469–2527
5. Zhang ZJ, Wang J, Chen CH (2013) Near-infrared light-mediated nanoplatforms for cancer thermo-chemotherapy and optical imaging. Adv Mater 25:3869–3880
6. Vahrmeijer AL, Hutteman M, van der Vorst JR et al (2013) Image-guided cancer surgery using near-infrared fluorescence. Nat Rev Clin Oncol 10:507–518
7. Gioux S, Choi HS, Frangioni JV (2010) Image-guided surgery using invisible near-infrared light: fundamentals of clinical translation. Mol Imaging 9:237–255
8. Handgraaf HJ, Verbeek FP, Tummers QR et al (2014) Real-time near-infrared fluorescence guided surgery in gynecologic oncology: a review of the current state of the art. Gynecol Oncol 135:606–613
9. Mohajerani P, Adibi A, Kempner J, Yared W (2009) Compensation of optical heterogeneity-induced artifacts in fluorescence molecular tomography: theory and in vivo validation. J Biomed Opt 14:034021
10. Wang LHV, Hu S (2012) Photoacoustic tomography: in vivo imaging from organelles to organs. Science 335:1458–1462
11. Michalet X, Pinaud FF, Bentolila LA et al (2005) Quantum dots for live cells, in vivo imaging, and diagnostics. Science 307:538–544
12. Li LL, Wu GH, Yang GH et al (2013) Focusing on luminescent graphene quantum dots: current status and future perspectives. Nanoscale 5:4015–4039

13. Cao-Milan R, Liz-Marzan LM (2014) Gold nanoparticle conjugates: recent advances toward clinical applications. Expert Opin Drugs Deliv 11:741–752
14. Gong H, Peng R, Liu Z (2013) Carbon nanotubes for biomedical imaging: the recent advances. Adv Drugs Deliv Rev 65:1951–1963
15. Liu YS, Tu DT, Zhu HM, Chen XY (2013) Lanthanide-doped luminescent nanoprobes: controlled synthesis, optical spectroscopy, and bioapplications. Chem Soc Rev 42:6924–6958
16. Wang X, Lv JZ, Yao XY et al (2014) Screening and investigation of a cyanine fluorescent probe for simultaneous sensing of glutathione and cysteine under single excitation. Chem Commun 50:15439–15442
17. Alivisatos AP (1996) Semiconductor clusters, nanocrystals, and quantum dots. Science 271:933–937
18. Alivisatos P (2004) The use of nanocrystals in biological detection. Nat Biotechnol 22:47–52
19. Gao X, Cui Y, Levenson RM et al (2004) In vivo cancer targeting and imaging with semiconductor quantum dots. Nat Biotechnol 22:969–976
20. Kim S, Lim YT, Soltesz EG et al (2004) Near-infrared fluorescent type II quantum dots for sentinel lymph node mapping. Nat Biotechnol 22:93–97
21. Smith AM, Duan H, Mohs AM, Nie S (2008) Bioconjugated quantum dots for in vivo molecular and cellular imaging. Adv Drugs Deliv Rev 60:1226–1240
22. Zrazhevskiy P, True LD, Gao XH (2013) Multicolor multicycle molecular profiling with quantum dots for single-cell analysis. Nat Protoc 8:1852–1869
23. Benito-Alifonso D, Tremel S, Hou B et al (2014) Lactose as a "Trojan Horse" for quantum dot cell transport. Angew Chem Int Ed 53:810–814
24. Bailey RE, Nie S (2003) Alloyed semiconductor quantum dots: tuning the optical properties without changing the particle size. J Am Chem Soc 125:7100–7106
25. Hines MA, Scholes GD (2003) Colloidal PbS nanocrystals with size-tunable near-infrared emission: observation of post-synthesis self-narrowing of the particle size distribution. Adv Mater 15:1844–1849
26. Zhong X, Feng Y, Knoll W, Han M (2003) Alloyed Zn(x)Cd(1-x)S nanocrystals with highly narrow luminescence spectral width. J Am Chem Soc 125:13559–13563
27. Nakane Y, Tsukasaki Y, Sakata T et al (2013) Aqueous synthesis of glutathione-coated PbS quantum dots with tunable emission for non-invasive fluorescence imaging in the second near-infrared biological window (1000–1400 nm). Chem Commun 49:7584–7586
28. Dabbousi BO, RodriguezViejo J, Mikulec FV et al (1997) (CdSe)ZnS core-shell quantum dots: synthesis and characterization of a size series of highly luminescent nanocrystallites. J Phys Chem B 101:9463–9475
29. Hines MA, Guyot-Sionnest P (1996) Synthesis and characterization of strongly luminescing ZnS-capped CdSe nanocrystals. J Phys Chem-Us 100:468–471
30. Kim S, Fisher B, Eisler HJ, Bawendi M (2003) Type-II quantum dots: CdTe/CdSe(core/shell) and CdSe/ZnTe(core/shell) heterostructures. J Am Chem Soc 125:11466–11467
31. Pietryga JM, Schaller RD, Werder D et al (2004) Pushing the band gap envelope: mid-infrared emitting colloidal PbSe quantum dots. J Am Chem Soc 126:11752–11753
32. Qu L, Peng X (2002) Control of photoluminescence properties of CdSe nanocrystals in growth. J Am Chem Soc 124:2049–2055
33. Voura EB, Jaiswal JK, Mattoussi H, Simon SM (2004) Tracking metastatic tumor cell extravasation with quantum dot nanocrystals and fluorescence emission-scanning microscopy. Nat Med 10:993–998
34. Walker KAD, Morgan C, Doak SH, Dunstan PR (2012) Quantum dots for multiplexed detection and characterisation of prostate cancer cells using a scanning near-field optical microscope. PLoS One 7:e31592
35. Stroh M, Zimmer JP, Duda DG et al (2005) Quantum dots spectrally distinguish multiple species within the tumor milieu in vivo. Nat Med 11:678–682

36. Jaiswal JK, Mattoussi H, Mauro JM, Simon SM (2003) Long-term multiple color imaging of live cells using quantum dot bioconjugates. Nat Biotechnol 21:47–51
37. Medintz IL, Uyeda HT, Goldman ER, Mattoussi H (2005) Quantum dot bioconjugates for imaging, labelling and sensing. Nat Mater 4:435–446
38. Alivisatos AP, Gu W, Larabell C (2005) Quantum dots as cellular probes. Annu Rev Biomed Eng 7:55–76
39. Wu X, Liu H, Liu J et al (2003) Immunofluorescent labeling of cancer marker Her2 and other cellular targets with semiconductor quantum dots. Nat Biotechnol 21:41–46
40. Herod MR, Pineda RG, Mautner V, Onion D (2014) Quantum dot labelling of adenovirus allows highly sensitive single cell flow and imaging cytometry. Small
41. Cai WB, Shin DW, Chen K et al (2006) Peptide-labeled near-infrared quantum dots for imaging tumor vasculature in living subjects. Nano Lett 6:669–676
42. Chen Y, Molnar M, Li L et al (2013) Characterization of VCAM-1-binding peptide-functionalized quantum dots for molecular imaging of inflamed endothelium. PLoS One 8:e83805
43. Ballou B, Ernst LA, Andreko S et al (2007) Sentinel lymph node imaging using quantum dots in mouse tumor models. Bioconjug Chem 18:389–396
44. Si C, Zhang Y, Lv X et al (2014) In vivo lymph node mapping by cadmium tellurium quantum dots in rats. J Surg Res 192:305–311
45. Akerman ME, Chan WC, Laakkonen P et al (2002) Nanocrystal targeting in vivo. Proc Natl Acad Sci U S A 99:12617–12621
46. Nurunnabi M, Cho KJ, Choi JS et al (2010) Targeted near-IR QDs-loaded micelles for cancer therapy and imaging. Biomaterials 31:5436–5444
47. Murray CB, Norris D, Bawendi MG (1993) Synthesis and characterization of nearly monodisperse CdE (E = S, Se, Te) semiconductor nanocrystallites. J Am Chem Soc 115:8706–8715
48. Talapin DV, Rogach AL, Kornowski A, Haase M, Weller H (2001) Highly luminescent monodisperse CdSe and CdSe/ZnS nanocrystals synthesized in a hexadecylamine-trioctylphosphine oxide-trioctylphosphine mixture. Nano Lett 1:207–211
49. Yu WW, Qu LH, Guo WZ, Peng XG (2003) Experimental determination of the extinction coefficient of CdTe, CdSe, and CdS nanocrystals. Chem Mater 15:2854–2860
50. Xie R, Kolb U, Li J et al (2005) Synthesis and characterization of highly luminescent CdSe-core CdS/Zn0.5Cd0.5S/ZnS multishell nanocrystals. J Am Chem Soc 127:7480–7488
51. Pons T, Pic E, Lequeux N et al (2010) Cadmium-free CuInS2/ZnS quantum dots for sentinel lymph node imaging with reduced toxicity. ACS Nano 4:2531–2538
52. Zheng XT, Ananthanarayanan A, Luo KQ, Chen P (2014) Glowing graphene quantum dots and carbon dots: properties, syntheses, and biological applications. Small
53. Wang L, Wang Y, Xu T et al (2014) Gram-scale synthesis of single-crystalline graphene quantum dots with superior optical properties. Nat Commun 5:5357
54. Chen XX, Jin QQ, Wu LZ et al (2014) Synthesis and unique photoluminescence properties of nitrogen-rich quantum dots and their applications. Angew Chem Int Ed 53:12542–12547
55. Chan WC, Nie S (1998) Quantum dot bioconjugates for ultrasensitive nonisotopic detection. Science 281:2016–2018
56. Bruchez M Jr, Moronne M, Gin P et al (1998) Semiconductor nanocrystals as fluorescent biological labels. Science 281:2013–2016
57. Pinaud F, King D, Moore HP, Weiss S (2004) Bioactivation and cell targeting of semiconductor CdSe/ZnS nanocrystals with phytochelatin-related peptides. J Am Chem Soc 126:6115–6123
58. Huang BH, Tomalia DA (2005) Dendronization of gold and CdSe/cdS (core-shell) quantum functionalized dendrons dots with tomalia type, thiol core, poly(amidoamine) (PAMAM) dendrons. J Lumin 111:215–223
59. Kim S, Bawendi MG (2003) Oligomeric ligands for luminescent and stable nanocrystal quantum dots. J Am Chem Soc 125:14652–14653

60. Kirchner C, Javier AM, Susha AS et al (2005) Cytotoxicity of nanoparticle-loaded polymer capsules. Talanta 67:486–491
61. Gerion D, Pinaud F, Williams SC et al (2001) Synthesis and properties of biocompatible water-soluble silica-coated CdSe/ZnS semiconductor quantum dots. J Phys Chem B 105:8861–8871
62. Dubertret B, Skourides P, Norris DJ et al (2002) In vivo imaging of quantum dots encapsulated in phospholipid micelles. Science 298:1759–1762
63. Larson DR, Zipfel WR, Williams RM et al (2003) Water-soluble quantum dots for multiphoton fluorescence imaging in vivo. Science 300:1434–1436
64. Mattoussi H, Mauro JM, Goldman ER et al (2000) Self-assembly of CdSe-ZnS quantum dot bioconjugates using an engineered recombinant protein. J Am Chem Soc 122:12142–12150
65. Liu TC, Zhang HL, Wang JH et al (2008) Study on molecular interactions between proteins on live cell membranes using quantum dot-based fluorescence resonance energy transfer. Anal Bioanal Chem 391:2819–2824
66. Xing Y, Chaudry Q, Shen C et al (2007) Bioconjugated quantum dots for multiplexed and quantitative immunohistochemistry. Nat Protoc 2:1152–1165
67. Lee J, Choi Y, Kim K et al (2010) Characterization and cancer cell specific binding properties of anti-EGFR antibody conjugated quantum dots. Bioconjug Chem 21:940–946
68. Hafian H, Sukhanova A, Turini M et al (2014) Multiphoton imaging of tumor biomarkers with conjugates of single-domain antibodies and quantum dots. Nanomed Nanotechnol 10:1701–1709
69. Rakovich TY, Mahfoud OK, Mohamed BM et al (2014) Highly sensitive single domain antibody-quantum dot conjugates for detection of HER2 biomarker in lung and breast cancer cells. ACS Nano 8:5682–5695
70. Anas A, Okuda T, Kawashima N et al (2009) Clathrin-mediated endocytosis of quantum dot-peptide conjugates in living cells. ACS Nano 3:2419–2429
71. Duan HW, Nie SM (2007) Cell-penetrating quantum dots based on multivalent and endosome-disrupting surface coatings. J Am Chem Soc 129:3333–3338
72. Bakalova R, Ohba H, Zhelev Z et al (2004) Quantum dot anti-CD conjugates: are they potential photosensitizers or potentiators of classical photosensitizing agents in photodynamic therapy of cancer? Nano Lett 4:1567–1573
73. Chen XC, Deng YL, Lin Y et al (2008) Quantum dot-labeled aptamer nanoprobes specifically targeting glioma cells. Nanotechnology 19:235105
74. Zhang J, Jia X, Lv XJ et al (2010) Fluorescent quantum dot-labeled aptamer bioprobes specifically targeting mouse liver cancer cells. Talanta 81:505–509
75. Zhang MZ, Yu RN, Chen J et al (2012) Targeted quantum dots fluorescence probes functionalized with aptamer and peptide for transferrin receptor on tumor cells. Nanotechnology 23:485104
76. Patt M, Schildan A, Habermann B et al (2010) F-18- and C-11-labelling of quantum dots with n.c.a. [F-18]fluoroethyltosylate and [C-11]methyliodide: a feasibility study. J Radioanal Nucl Chem 283:487–491
77. Cai WB, Chen K, Li ZB et al (2007) Dual-function probe for PET and near-infrared fluorescence imaging of tumor vasculature. J Nucl Med 48:1862–1870
78. Sun X, Huang X, Guo J et al (2014) Self-illuminating 64Cu-doped CdSe/ZnS nanocrystals for in vivo tumor imaging. J Am Chem Soc 136:1706–1709
79. Fan HM, Olivo M, Shuter B et al (2010) Quantum dot capped magnetite nanorings as high performance nanoprobe for multiphoton fluorescence and magnetic resonance imaging. J Am Chem Soc 132:14803–14811
80. Jing LH, Ding K, Kershaw SV et al (2014) Magnetically engineered semiconductor quantum dots as multimodal imaging probes. Adv Mater 26:6367–6386
81. Chakravarthy KV, Davidson BA, Helinski JD et al (2010) Doxorubicin-conjugated quantum dots to target alveolar macrophages and inflammation. Nanomedicine

82. Jung J, Solanki A, Memoli KA et al (2010) Selective inhibition of human brain tumor cells through multifunctional quantum-dot-based siRNA delivery. Angew Chem Int Ed Engl 49:103–107
83. Ho YP, Leong KW (2010) Quantum dot-based theranostics. Nanoscale 2:60–68
84. Li JM, Wang YY, Zhao MX et al (2012) Multifunctional QD-based co-delivery of siRNA and doxorubicin to HeLa cells for reversal of multidrug resistance and real-time tracking. Biomaterials 33:2780–2790
85. Ryman-Rasmussen JP, Riviere JE, Monteiro-Riviere NA (2007) Surface coatings determine cytotoxicity and irritation potential of quantum dot nanoparticles in epidermal keratinocytes. J Invest Dermatol 127:143–153
86. Zhang TT, Stilwell JL, Gerion D et al (2006) Cellular effect of high doses of silica-coated quantum dot profiled with high throughput gene expression analysis and high content cellomics measurements. Nano Lett 6:800–808
87. Gao X, Yang L, Petros JA et al (2005) In vivo molecular and cellular imaging with quantum dots. Curr Opin Biotechnol 16:63–72
88. Smith RA, Giorgio TD (2009) Quantitative measurement of multifunctional quantum dot binding to cellular targets using flow cytometry. Cytom Part A 75A:465–474
89. Mathur A, Kelso DM (2010) Multispectral image analysis of binary encoded microspheres for highly multiplexed suspension arrays. Cytometry A 77:356–365
90. Prasuhn DE, Feltz A, Blanco-Canosa JB et al (2010) Quantum dot peptide biosensors for monitoring caspase 3 proteolysis and calcium ions. ACS Nano 4:5487–5497
91. He X, Li Z, Chen M, Ma N (2014) DNA-programmed dynamic assembly of quantum dots for molecular computation. Angew Chem 53:14447–14450
92. Chen K, Li ZB, Wang H et al (2008) Dual-modality optical and positron emission tomography imaging of vascular endothelial growth factor receptor on tumor vasculature using quantum dots. Eur J Nucl Med Mol Imaging 35:2235–2244
93. Yoshioka T, Mishima H, Kaul Z et al (2010) Fate of bone marrow mesenchymal stem cells following the allogeneic transplantation of cartilaginous aggregates into osteochondral defects of rabbits. J Tissue Eng Regen Med
94. Liu J, Lau SK, Varma VA et al (2010) Multiplexed detection and characterization of rare tumor cells in Hodgkin's lymphoma with multicolor quantum dots. Anal Chem 82:6237–6243
95. Papagiannaros A, Upponi J, Hartner W et al (2010) Quantum dot-loaded immunomicelles for tumor imaging. BMC Med Imaging 10:22
96. Al-Jamal WT, Al-Jamal KT, Tian B et al (2009) Tumor targeting of functionalized quantum dot-liposome hybrids by intravenous administration. Mol Pharm 6:520–530
97. Lu Y, Zhong Y, Wang J et al (2013) Aqueous synthesized near-infrared-emitting quantum dots for RGD-based in vivo active tumour targeting. Nanotechnology 24:135101
98. Mulder WJM, Koole R, Brandwijk RJ et al (2006) Quantum dots with a paramagnetic coating as a bimodal molecular imaging probe. Nano Lett 6:1–6
99. van Tilborg GAF, Mulder WJM, Chin PTK et al (2006) Annexin A5-conjugated quantum dots with a paramagnetic lipidic coating for the multimodal detection of apoptotic cells. Bioconjug Chem 17:865–868
100. Schipper ML, Cheng Z, Lee SW et al (2007) MicroPET-based biodistribution of quantum dots in living mice. J Nucl Med 48:1511–1518
101. Cai WB, Chen XY (2007) Nanoplatforms for targeted molecular imaging in living subjects. Small 3:1840–1854
102. Ballou B, Lagerholm BC, Ernst LA et al (2004) Noninvasive imaging of quantum dots in mice. Bioconjug Chem 15:79–86
103. Choi HS, Ipe BI, Misra P et al (2009) Tissue- and organ-selective biodistribution of NIR fluorescent quantum dots. Nano Lett 9:2354–2359

104. Fischer HC, Liu LC, Pang KS, Chan WCW (2006) Pharmacokinetics of nanoscale quantum dots: in vivo distribution, sequestration, and clearance in the rat. Adv Funct Mater 16:1299–1305
105. Choi AO, Cho SJ, Desbarats J et al (2007) Quantum dot-induced cell death involves Fas upregulation and lipid peroxidation in human neuroblastoma cells. J Nanobiotechnol 5:1
106. Schipper ML, Iyer G, Koh AL et al (2009) Particle size, surface coating, and PEGylation influence the biodistribution of quantum dots in living mice. Small 5:126–134
107. Gopee NV, Roberts DW, Webb P et al (2007) Migration of intradermally injected quantum dots to sentinel organs in mice. Toxicol Sci 98:249–257
108. Parungo CP, Colson YL, Kim SW et al (2005) Sentinel lymph node mapping of the pleural space. Chest 127:1799–1804
109. Parungo CP, Ohnishi S, Kim SW et al (2005) Intraoperative identification of esophageal sentinel lymph nodes with near-infrared fluorescence imaging. J Thorac Cardiovasc Surg 129:844–850
110. Soltesz EG, Kim S, Kim SW et al (2006) Sentinel lymph node mapping of the gastrointestinal tract by using invisible light. Ann Surg Oncol 13:386–396
111. Soltesz EG, Kim S, Laurence RG et al (2005) Intraoperative sentinel lymph node mapping of the lung using near-infrared fluorescent quantum dots. Ann Thorac Surg 79:269–277
112. Zimmer JP, Kim SW, Ohnishi S et al (2006) Size series of small indium arsenide-zinc selenide core-shell nanocrystals and their application to in vivo imaging. J Am Chem Soc 128:2526–2527
113. Yang RS, Chang LW, Wu JP et al (2007) Persistent tissue kinetics and redistribution of nanoparticles, quantum dot 705, in mice: ICP-MS quantitative assessment. Environ Health Perspect 115:1339–1343
114. Derfus AM, Chan WC, Bhatia SN (2003) Probing the cytotoxicity of semiconductor quantum dots. Nano Lett 4:11–18
115. Kirchner C, Liedl T, Kudera S et al (2005) Cytotoxicity of colloidal CdSe and CdSe/ZnS nanoparticles. Nano Lett 5:331–338
116. Clarke SJ, Hollmann CA, Zhang Z et al (2006) Photophysics of dopamine-modified quantum dots and effects on biological systems. Nat Mater 5:409–417
117. Lovric J, Bazzi HS, Cuie Y et al (2005) Differences in subcellular distribution and toxicity of green and red emitting CdTe quantum dots. J Mol Med 83:377–385
118. Cho SJ, Maysinger D, Jain M et al (2007) Long-term exposure to CdTe quantum dots causes functional impairments in live cells. Langmuir 23:1974–1980
119. Hoshino A, Fujioka K, Oku T et al (2004) Physicochemical properties and cellular toxicity of nanocrystal quantum dots depend on their surface modification. Nano Lett 4:2163–2169
120. Lovric J, Cho SJ, Winnik FM, Maysinger D (2005) Unmodified cadmium telluride quantum dots induce reactive oxygen species formation leading to multiple organelle damage and cell death. Chem Biol 12:1227–1234
121. Shiohara A, Hoshino A, Hanaki K et al (2004) On the cyto-toxicity caused by quantum dots. Microbiol Immunol 48:669–675
122. Boldt K, Bruns OT, Gaponik N, Eychmuller A (2006) Comparative examination of the stability of semiconductor quantum dots in various biochemical buffers. J Phys Chem B 110:1959–1963
123. Dollefeld H, Hoppe K, Kolny J et al (2002) Investigations on the stability of thiol stabilized semiconductor nanoparticles. Phys Chem Chem Phys 4:4747–4753
124. Pellegrino T, Manna L, Kudera S et al (2004) Hydrophobic nanocrystals coated with an amphiphilic polymer shell: a general route to water soluble nanocrystals. Nano Lett 4:703–707
125. Chen FQ, Gerion D (2004) Fluorescent CdSe/ZnS nanocrystal-peptide conjugates for long-term, nontoxic imaging and nuclear targeting in living cells. Nano Lett 4:1827–1832
126. Rieger S, Kulkarni RP, Darcy D et al (2005) Quantum dots are powerful multipurpose vital labeling agents in zebrafish embryos. Dev Dyn 234:670–681

127. Manabe N, Hoshino A, Liang YQ et al (2006) Quantum dot as a drug tracer in vivo. IEEE Trans Nanobiosci 5:263–267
128. Stroh M, Zimmer JP, Duda DG et al (2005) Quantum dots spectrally distinguish multiple species within the tumor milieu in vivo. Nat Mater 11:678–682
129. Ho YP, Chen HH, Leong KW, Wang TH (2006) Evaluating the intracellular stability and unpacking of DNA nanocomplexes by quantum dots-FRET. J Control Release 116:83–89
130. Chen HH, Ho YP, Jiang X et al (2009) Simultaneous non-invasive analysis of DNA condensation and stability by two-step QD-FRET. Nano Today 4:125–134
131. Zhang BQ, Zhang YJ, Mallapragada SK, Clapp AR (2011) Sensing polymer/DNA polyplex dissociation using quantum dot fluorophores. ACS Nano 5:129–138
132. Anas A, Akita H, Harashima H et al (2008) Photosensitized breakage and damage of DNA by CdSe-ZnS quantum dots. J Phys Chem B 112:10005–10011
133. Srinivasan C, Lee J, Papadimitrakopoulos F et al (2006) Labeling and intracellular tracking of functionally active plasmid DNA with semiconductor quantum dots. Mol Ther: J Am Soc Genet Ther 14:192–201
134. Li D, Li G, Guo W et al (2008) Glutathione-mediated release of functional plasmid DNA from positively charged quantum dots. Biomaterials 29:2776–2782
135. Zintchenko A, Susha AS, Concia M et al (2009) Drug nanocarriers labeled with near-infrared-emitting quantum dots (quantoplexes): imaging fast dynamics of distribution in living animals. Mol Ther: J Am Soc Genet Ther 17:1849–1856
136. Derfus AM, Chen AA, Min DH et al (2007) Targeted quantum dot conjugates for siRNA delivery. Bioconjug Chem 18:1391–1396
137. Chen AA, Derfus AM, Khetani SR, Bhatia SN (2005) Quantum dots to monitor RNAi delivery and improve gene silencing. Nucleic Acids Res 33:e190
138. Tan WB, Jiang S, Zhang Y (2007) Quantum-dot based nanoparticles for targeted silencing of HER2/neu gene via RNA interference. Biomaterials 28:1565–1571
139. Jung JJ, Solanki A, Memoli KA et al (2010) Selective inhibition of human brain tumor cells through multifunctional quantum-dot-based siRNA delivery. Angew Chem Int Ed 49:103–107
140. Walther C, Meyer K, Rennert R, Neundorf I (2008) Quantum dot-carrier peptide conjugates suitable for imaging and delivery applications. Bioconjug Chem 19:2346–2356
141. Yezhelyev MV, Qi L, O'Regan RM et al (2008) Proton-sponge coated quantum dots for siRNA delivery and intracellular imaging. J Am Chem Soc 130:9006–9012
142. Qi L, Gao X (2008) Quantum dot-amphipol nanocomplex for intracellular delivery and real-time imaging of siRNA. ACS Nano 2:1403–1410
143. Rowe MD, Thamm DH, Kraft SL, Boyes SG (2009) Polymer-modified gadolinium metal-organic framework nanoparticles used as multifunctional nanomedicines for the targeted imaging and treatment of cancer. Biomacromolecules 10:983–993
144. Kim K, Kim JH, Park H et al (2010) Tumor-homing multifunctional nanoparticles for cancer theragnosis: simultaneous diagnosis, drug delivery, and therapeutic monitoring. J Control Release 146:219–227
145. Bagalkot V, Zhang L, Levy-Nissenbaum E et al (2007) Quantum dot – aptamer conjugates for synchronous cancer imaging, therapy, and sensing of drug delivery based on bi-fluorescence resonance energy transfer. Nano Lett 7:3065–3070
146. Weng KC, Noble CO, Papahadjopoulos-Sternberg B et al (2008) Targeted tumor cell internalization and imaging of multifunctional quantum dot-conjugated immunoliposomes in vitro and in vivo. Nano Lett 8:2851–2857
147. Tian B, Al-Jamal WT, Al-Jamal KT, Kostarelos K (2011) Doxorubicin-loaded lipid-quantum dot hybrids: surface topography and release properties. Int J Pharm 416:443–447
148. Al-Jamal WT, Al-Jamal KT, Tian B et al (2008) Lipid-quantum dot bilayer vesicles enhance tumor cell uptake and retention in vitro and in vivo. ACS Nano 2:408–418
149. Al-Jamal WT, Al-Jamal KT, Bomans PH et al (2008) Functionalized-quantum-dot-liposome hybrids as multimodal nanoparticles for cancer. Small 4:1406–1415

150. Gopalakrishnan G, Danelon C, Izewska P et al (2006) Multifunctional lipid/quantum dot hybrid nanocontainers for controlled targeting of live cells. Angew Chem 45:5478–5483
151. Erogbogbo F, Yong KT, Hu R et al (2010) Biocompatible magnetofluorescent probes: luminescent silicon quantum dots coupled with superparamagnetic iron (III) oxide. ACS Nano 4:5131–5138
152. Nair LV, Nagaoka Y, Maekawa T et al (2014) Quantum dot tailored to single wall carbon nanotubes: a multifunctional hybrid nanoconstruct for cellular imaging and targeted photothermal therapy. Small 10:2771–2775, 2740
153. Shi DL, Cho HS, Huth C et al (2009) Conjugation of quantum dots and Fe3O4 on carbon nanotubes for medical diagnosis and treatment. Appl Phys Lett 95:223702
154. Park JH, von Maltzahn G, Ruoslahti E et al (2008) Micellar hybrid nanoparticles for simultaneous magnetofluorescent imaging and drug delivery. Angew Chem 47:7284–7288
155. Zhou Y, Shi L, Li Q et al (2010) Imaging and inhibition of multi-drug resistance in cancer cells via specific association with negatively charged CdTe quantum dots. Biomaterials 31:4958–4963
156. Juzenas P, Chen W, Sun YP et al (2008) Quantum dots and nanoparticles for photodynamic and radiation therapies of cancer. Adv Drug Deliv Rev 60:1600–1614
157. Martynenko IV, Kuznetsova VA, Orlova AC et al (2015) Chlorin e6-ZnSe/ZnS quantum dots based system as reagent for photodynamic therapy. Nanotechnology 26:055102
158. Yaghini E, Seifalian AM, MacRobert AJ (2009) Quantum dots and their potential biomedical applications in photosensitization for photodynamic therapy. Nanomedicine (Lond) 4:353–363